

Disorder effects in NbTiN superconducting resonators

Wei-Tao Lyu(吕伟涛), Qiang Zhi(支强), Jie Hu(胡洁), Jing Li(李婧), and Sheng-Cai Shi(史生才)

Citation: Chin. Phys. B, 2024, 33 (**2**): 027401. DOI: 10.1088/1674-1056/ad03dc
Journal homepage: http://cpb.iphy.ac.cn; http://iopscience.iop.org/cpb

What follows is a list of articles you may be interested in

Role of grain boundary networks in vortex motion in superconducting films

Yu Liu(刘宇), Feng Xue(薛峰), and Xiao-Fan Gou(苟晓凡)
Chin. Phys. B, 2023, 32 (**12**): 127401. DOI: 10.1088/1674-1056/ace315

Flux pinning evolution in multilayer Pb/Ge/Pb/Ge/Pb superconducting systems

Li-Xin Gao(高礼鑫), Xiao-Ke Zhang(张晓珂), An-Lei Zhang(张安蕾), Qi-Ling Xiao(肖祁陵), Fei Chen(陈飞), and Jun-Yi Ge(葛军饴)
Chin. Phys. B, 2023, 32 (**3**): 037402. DOI: 10.1088/1674-1056/ac89e1

Wire network behavior of superconducting films with lower symmetrical mesoscopic hole arrays

Wei-Gui Guo(郭伟贵), Zi-Xi Pei(裴子玺), and Xiang-Gang Qiu(邱祥冈)
Chin. Phys. B, 2022, 31 (**3**): 037405. DOI: 10.1088/1674-1056/ac43af

Investigation of dimensionality in superconducting NbN thin film samples with different thicknesses and NbTiN meander nanowire samples by measuring the upper critical field

Mudassar Nazir, Xiaoyan Yang(杨晓燕), Huanfang Tian(田焕芳), Pengtao Song(宋鹏涛), Zhan Wang(王战), Zhongcheng Xiang(相忠诚), Xueyi Guo(郭学仪), Yirong Jin(金贻荣), Lixing You(尤立星), Dongning Zheng(郑东宁)
Chin. Phys. B, 2020, 29 (**8**): 087401. DOI: 10.1088/1674-1056/ab9740

High quality NbTiN films fabrication and rapid thermal annealing investigation

Huan Ge(葛欢), Yi-Rong Jin(金贻荣), Xiao-Hui Song(宋小会)
Chin. Phys. B, 2019, 28 (**7**): 077402. DOI: 10.1088/1674-1056/28/7/077402

Disorder effects in NbTiN superconducting resonators

Wei-Tao Lyu(吕伟涛)[1], Qiang Zhi(支强)[1], Jie Hu(胡洁)[2], Jing Li(李婧)[1], and Sheng-Cai Shi(史生才)[1,†]

[1] *Purple Mountain Observatory, Chinese Academy of Sciences, Nanjing* 210034, *China*
[2] *GEPI, Observatoire de Paris, PSL Université, CNRS, Paris* 75014, *France*

(Received 30 July 2023; revised manuscript received 13 October 2023; accepted manuscript online 17 October 2023)

Disordered superconducting materials like NbTiN possess a high kinetic inductance fraction and an adjustable critical temperature, making them a good choice for low-temperature detectors. Their energy gap (Δ), critical temperature (T_c), and quasiparticle density of states (QDOS) distribution, however, deviate from the classical BCS theory due to the disorder effects. The Usadel equation, which takes account of elastic scattering, non-elastic scattering, and electro–phonon coupling, can be applied to explain and describe these deviations. This paper presents numerical simulations of the disorder effects based on the Usadel equation to investigate their effects on the Δ, T_c, QDOS distribution, and complex conductivity of the NbTiN film. Furthermore, NbTiN superconducting resonators with coplanar waveguide (CPW) structures are fabricated and characterized at different temperatures to validate our numerical simulations. The pair-breaking parameter α and the critical temperature in the pure state T_c^P of our NbTiN film are determined from the experimental results and numerical simulations. This study has significant implications for the development of low-temperature detectors made of disordered superconducting materials.

Keywords: effects of disorder, NbTiN, superconducting film, Usadel equation, complex conductivity, superconducting resonator

PACS: 74.62.En, 74.78.–w, 85.25.Pb, 74.25.nn **DOI:** 10.1088/1674-1056/ad03dc

1. Introduction

Low-temperature superconducting materials such as NbTiN, as well as its parent compounds NbN and TiN, have attracted significant attention due to their potential applications in low-temperature detectors and circuit quantum electrodynamics. NbTiN and NbN possess a high Δ and T_c, making them ideal for implementation in superconductor–insulator–superconductor (SIS) mixers and hot-electron bolometer (HEB) mixers.[1–3] NbTiN and TiN are also promising candidates for microwave kinetic inductance detectors (MKIDs) because of an adjustable T_c and large kinetic inductance fractions.[4,5] Moreover, NbTiN and NbN are well suited for applications in circuit quantum electrodynamics due to a high T_c and Δ, particularly in environments with strong magnetic fields.[6] These superconducting materials, however, are not immune to disorder effects on their basic parameters, such as the Δ, T_c, and QDOS distribution.[7–10] One kind of disorder effect, named magnetic impurities, in materials is reported to lead to the transformation of superconductors into insulators,[11] the appearance of pseudo-energy gaps, and the enhancement of pair-breaking effects in materials.[12,13] The generalized Usadel equation, which takes account of elastic scattering, non-elastic scattering, and electro–phonon coupling, is often introduced to solve diffusion, interface, and pair-breaking effects.[14] Here, we introduce the Usadel equation to simulate and describe the disorder effects in superconducting materials.

In this paper, we firstly introduce the Usadel equation and the related complex conductivity formulas. Then, we present numerical simulations by taking into consideration the Usadel equation to investigate the disorder effects on the Δ, T_c, QDOS, and complex conductivity of NbTiN superconducting film. Finally, we describe the experimental methodology by characterizing the disorder effects in NbTiN superconducting resonators.

2. Complex conductivity based on Usadel equation

The Usadel equation — a simplified version of the Eilenberger equation[15] — offers a more general and non-linear approach to describe superconductivity under the diffusion limit.[16] The superconducting state is described by the pairing angle $\theta(x,E)$, which is a complex function depending on space (x) and excited energy (E), in the Usadel equation. The variable θ ranges in magnitude from 0 to $\pi/2$, while $\theta = 0$ corresponds to the normal state. The QDOS of superconducting materials is $N_{qp} = N_0 \mathrm{Re}(\cos\theta)$, where N_0 is the QDOS in the normal state at the Fermi energy. The Usadel equation in one dimension and equilibrium can be expressed as[14]

$$\frac{\hbar D_S}{2}\frac{\partial^2\theta}{\partial x^2} + \mathrm{i}E\sin\theta - \left[\frac{\hbar}{\tau_{sf}} + \frac{\hbar D_S}{2}\left(\frac{\partial\varphi}{\partial x} + \frac{2e}{\hbar}A_x\right)^2\right]\cos\theta\sin\theta$$

†Corresponding author. E-mail: scshi@pmo.ac.cn

© 2024 Chinese Physical Society and IOP Publishing Ltd

$$+\Delta(x)\cos\theta = 0, \tag{1}$$

with

$$\Delta(x) = n_s V_{\text{eff}} \int_0^{\hbar\omega_D} \tanh(E/2k_BT)\,\text{Im}(\sin\theta)\,dE, \tag{2}$$

where V_{eff} is the BCS-like interaction potential, $\hbar\omega_D$ is the Debye energy, D_S is the diffusivity constant, τ_{sf} is the spin-flip time, φ is the usual superconducting phase, A_x is the vector potential, and Δ is the energy gap. The first term in Eq. (1) describes the diffusion in superconductors, which is often included in interface problems.[17] The second and fourth terms describe respective energies of excitation and pairing interactions, the same as the BCS description. The third term in Eq. (1) describes the pair-breaking effects, which can lead to the smearing of coherence peaks in the QDOS and the reduction of the Δ. As we focus on the study of the pair-breaking effects of superconducting materials, i.e., no diffusion and interface issues, Eq. (1) can be simplified with $D_S = 0$ as follows:

$$iE\sin\theta - \alpha\cos\theta\sin\theta + \Delta(x)\cos\theta = 0, \tag{3}$$

where α is the pair-breaking parameter.

The complex conductivity $\sigma = \sigma_1 + i\sigma_2$ is a crucial parameter for calculating the surface impedance of a superconducting film and characterizing electromagnetic responses of superconducting detectors. The classical superconductors' complex conductivity was originally derived by Mattis and Bardeen,[18] and later extended by Nam to the Green's function form of the pairing angle.[19] The extended version is written as

$$\begin{aligned}\hbar\omega\frac{\sigma_1}{\sigma_n} &= \int_{E_g-\hbar\omega}^{-E_g} dE g_1(E,E')\left[1-2f(E')\right] \\ &\quad +2\int_{E_g}^{\infty} dE g_1(E,E')\left[f(E)-f(E')\right], \end{aligned}\tag{4}$$

$$\begin{aligned}\hbar\omega\frac{\sigma_2}{\sigma_n} &= \int_{\max(E_g-\hbar\omega,-E_g)}^{\infty} dE g_2(E,E')\left[1-2f(E')\right] \\ &\quad +\int_{E_g}^{\infty} dE g_2(E',E)\left[1-2f(E)\right], \end{aligned}\tag{5}$$

where $E' = E+\hbar\omega$, $f(E)$ is the Fermi distribution function, $g_1(E,E') = \text{Re}[\cos\theta(E)]\cdot\text{Re}[\cos\theta(E')] + \text{Re}[i\sin\theta(E)]\times\text{Re}[i\sin\theta(E')]$, and $g_2(E,E') = \text{Im}[\cos\theta(E)]\cdot\text{Re}[\cos\theta(E')] + \text{Im}[i\sin\theta(E)]\cdot\text{Re}[i\sin\theta(E')]$. In the absence of pair-breaking effects ($\alpha = 0$), Eqs. (4) and (5) can be simplified to the classical complex conductivity formulas.

3. Numerical simulations for disorder effects

To understand the disorder effects on the characteristics of superconducting films, it is essential to simulate their effects on key parameters, such as the Δ, T_c, QDOS, and complex conductivity. Disordered superconductors exhibit a phenomenon known as the smearing of the coherence peak in the QDOS distribution, described by the function of $\cos\theta$. The pair-breaking parameter α is introduced in the Usadel equation to account for the disorder effects in superconducting films. The larger α is, the lower and broader the coherence peak ($E = \Delta$) in the QDOS distribution becomes. To obtain the QDOS distribution of disordered superconducting materials, $\cos\theta$ needs to be solved from Eq. (3), which is essentially a quartic function about $\cos\theta$. By solving equations with the numerical solutions and considering the physical meaning of $\cos\theta$, we can calculate the complex functions $\cos\theta$ and $\sin\theta$ about E at a certain α.

Figure 1(a) illustrates the simulated results of QDOS distribution with respect to E for different values of α. Smearing of coherence peaks in the QDOS can be clearly seen, just as observed by reported results.[11] Figure 1(b) presents the distributions of $\cos\theta$ and $\sin\theta$ about E when $\alpha/\Delta = 0.05$. Our numerical simulation results, obtained by solving Eq. (3), further confirm that the pair-breaking effects in superconducting materials do result in a minimum excitation energy (E_g) that is smaller than, rather than equal to, the Δ. According to the Abrikosov and Gor'kov model, the relationship between the pair-breaking parameter α and the minimum excitation energy E_g is $E_g/\Delta = (1-(\alpha/\Delta)^{2/3})^{3/2}$.[20]

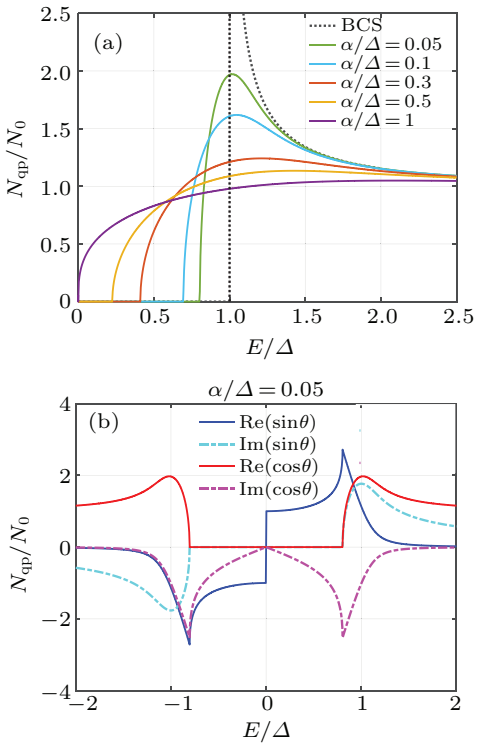


Fig. 1. (a) Simulated results of the distribution of the QDOS distribution with respect to E for different values of α. (b) An example of the real and imaginary parts of $\cos\theta$ and $\sin\theta$ distributions about E when $\alpha/\Delta = 0.05$.

As mentioned before, the Δ of superconducting materials also needs to be reevaluated in numerical simulations due to the pair-breaking effects. According to Eq. (2), Δ is related to the complex function $\sin\theta$. To solve Δ, we adopted

iterative approaches in simulations. Using the Matsubara representation, we rewrite the formulas of Δ and α in disordered superconducting materials as follows:[21,22]

$$\Delta\cos\theta(\omega_n)-\omega_n\sin\theta(\omega_n)-\alpha\sin\theta(\omega_n)\cos\theta(\omega_n)=0, \quad (6)$$

$$\Delta=2\pi k_{\rm B}T\sum_{n=0}^{\infty}(\sin\theta(\omega_n)\Big/\left[2\pi k_{\rm B}T\sum_{n=0}^{\infty}\left(\frac{1}{\omega_n}\right)-\ln\left(\frac{T_{\rm c}}{T}\right)\right], \quad (7)$$

where $\omega_n=(2n+1)\pi k_{\rm B}T$ are the Matsubara frequencies with $n=\{0,1,2,\ldots\}$. To solve Δ, we begin by guessing an initial value for Δ (here, we choose $1.76\cdot k_{\rm B}T_{\rm c}$). Next, we solve $\sin\theta(\omega_n)$ under all Matsubara frequencies using Eq. (6). We then substitute the solved $\sin\theta(\omega_n)$ into Eq. (7) to obtain an updated value of Δ until its convergence is achieved.

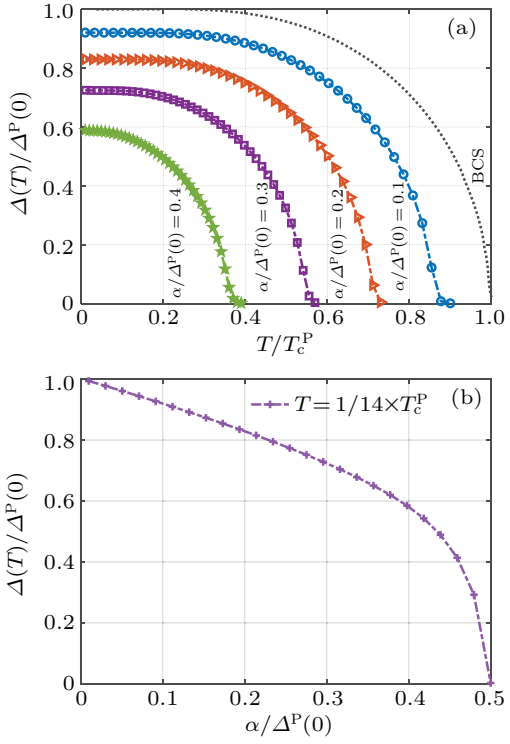


Fig. 2. (a) The simulated normalized energy gap $\Delta/\Delta^{\rm P}(0)$ with respect to the normalized temperature $T/T_{\rm c}^{\rm P}$ under different α. (b) Simulated results of the normalized energy gap $\Delta/\Delta^{\rm P}(0)$ with respect to α when $T=T_{\rm c}^{\rm P}/14$.

Figure 2(a) shows the dependence of the normalized energy gap $\Delta/\Delta^{\rm P}(0)$ upon the normalized temperature $T/T_{\rm c}^{\rm P}$ under different α. Here, $\Delta^{\rm P}$ and $T_{\rm c}^{\rm P}$ denote the Δ and $T_{\rm c}$ of superconducting materials in the absence of the pair-breaking effects (i.e., a pure system). In this figure, the dependence of Δ and T based on the BCS theory is also plotted for comparison. It can be seen clearly from Fig. 2(a) that as α increases, the $T_{\rm c}$ of superconducting materials decreases at a much faster rate than Δ at 0 K ($\Delta(0)$). Furthermore, the ratio $\Delta(0)/(k_{\rm B}T_{\rm c}^{\rm P})$ is no longer a constant with α increasing, as confirmed by reported scanning tunneling spectroscopy experiments.[23] Figure 2(b) shows the Δ of the superconducting materials as a function of α when $T=T_{\rm c}^{\rm P}/14$. As α increases, the Δ of the superconducting materials gradually decreases. When α exceeds $0.4\Delta^{\rm P}(0)$, the Δ of superconducting materials decreases rapidly and drops to zero at $0.5\Delta^{\rm P}(0)$, as predicted by Skalski.[11]

The simulated results indicate that pair-breaking effects have a negative correlation with the $T_{\rm c}$ of the superconducting materials. The results are in accordance with the pair-breaking theory introduced by Abrikosov and Gor'kov for magnetic impurities in a superconductor.[24,25] According to the theory, the $T_{\rm c}$ of the superconducting materials is written as

$$\ln\left(\frac{T_{\rm c}^{\rm P}}{T_{\rm c}}\right)=\psi\left(\frac{\alpha}{2\pi k_{\rm B}T_{\rm c}}+0.5\right)-\psi(0.5), \quad (8)$$

where ψ is the digamma function. We solve $T_{\rm c}$ via numerical iterations. The simulated results are shown in Fig. 3.

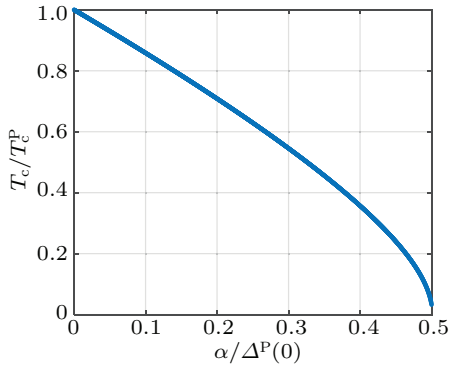


Fig. 3. Simulated results of the normalized temperature $T/T_{\rm c}^{\rm P}$ with respect to α.

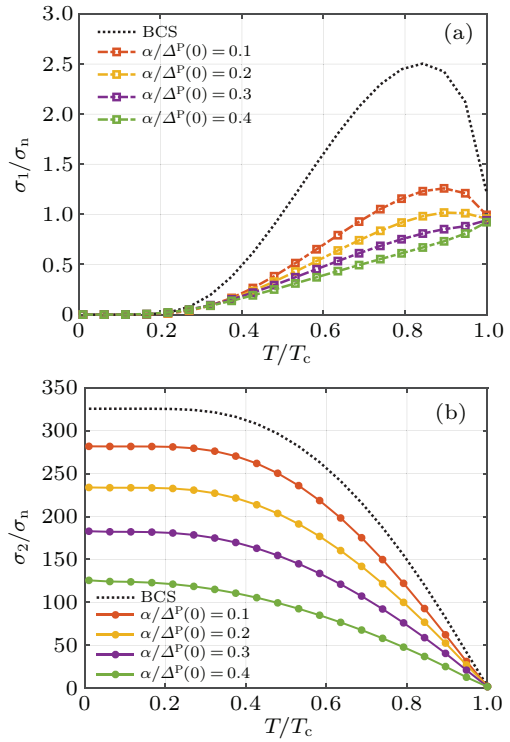


Fig. 4. Simulated results of σ_1 and σ_2 with respect to the normalized temperature $T/T_{\rm c}^{\rm P}$ for different α, assuming $f=5$ GHz and $T_{\rm c}^{\rm P}=14.1$ K. For reference, the dotted black line represents the simulated results using the BCS theory.

Once the T_c, Δ, and complex functions $\cos\theta$ and $\sin\theta$ are determined via numerical simulations, we can utilize Eqs. (4) and (5) to calculate the complex conductivity of the superconducting materials. This, in turn, enables us to derive various other electrical properties. Figure 4 presents the simulated complex conductivity of the superconducting materials at a frequency of 5 GHz and the T_c in a pure state of 14.1 K under different α. The dotted line represents the simulated results based on the BCS theory for comparison. From Fig. 4(a), we can see that as the temperature approaches the T_c, the real part of the complex conductivity approaches one. The degradation of superconductivity with the increasing pair-breaking level is also expected, as shown in Fig. 4(b).

4. Experimental characterization on NbTiN resonators

To validate our numerical simulations of superconducting materials in accounting for disorder effects, we chose NbTiN superconducting films as our subjects. To prepare our samples, we deposited a 130 nm thick NbTiN film on a 330 μm thick silicon wafer using reactive DC magnetron sputtering in a mixture of Ar and N_2. Using e-beam lithography and reactive ion etching techniques, we fabricated a set of 10 planar CPW resonators that were capacitively coupled to a straight feed line on the NbTiN film. The dimensions of the CPW resonators were carefully designed, with the center conductor and gap set at 3 μm and 2 μm, respectively. Similarly, the center conductor and gap of the CPW feed line were designed at 10 μm and 6 μm, respectively. The normal state sheet resistance R_s, measured at 15 K and T_c, is measured at 53.2 μΩ·cm and 14.1 K with our fridge, respectively.

The experimental sample, after cutting and cleaning, was mounted within a sealed gold-plated brass block connected to printed circuit boards (PCBs) with transition structures using aluminum wire bonding. The PCBs were then soldered to coaxial connectors for cable readouts. Beryllium copper pressure pads were employed to ensure an optimal thermal contact. The sample block was subsequently connected to an external vector network analyzer (VNA) through coaxial cables. Figure 5(a) provides a visual representation of the completed structures. Figure 5(b) depicts the installation of the sample on the 300 mK cold head of our adsorption refrigerator, as well as the setup and a diagram used during testing.

The transmission coefficient S_{21} of the feed line of the NbTiN sample at different temperatures was obtained using a heating device. Figure 5(c) illustrates the typical characteristics of one of the resonators, the absorption dip for different ambient temperatures. The temperature-dependent resonance characteristic is essentially induced by changes in complex conductivity, which can be expressed as $\delta f_0/f_0 = \alpha_{ki}\delta\sigma_2/(2\sigma_2)$, where α_{ki} is the kinetic inductance fraction.[26]

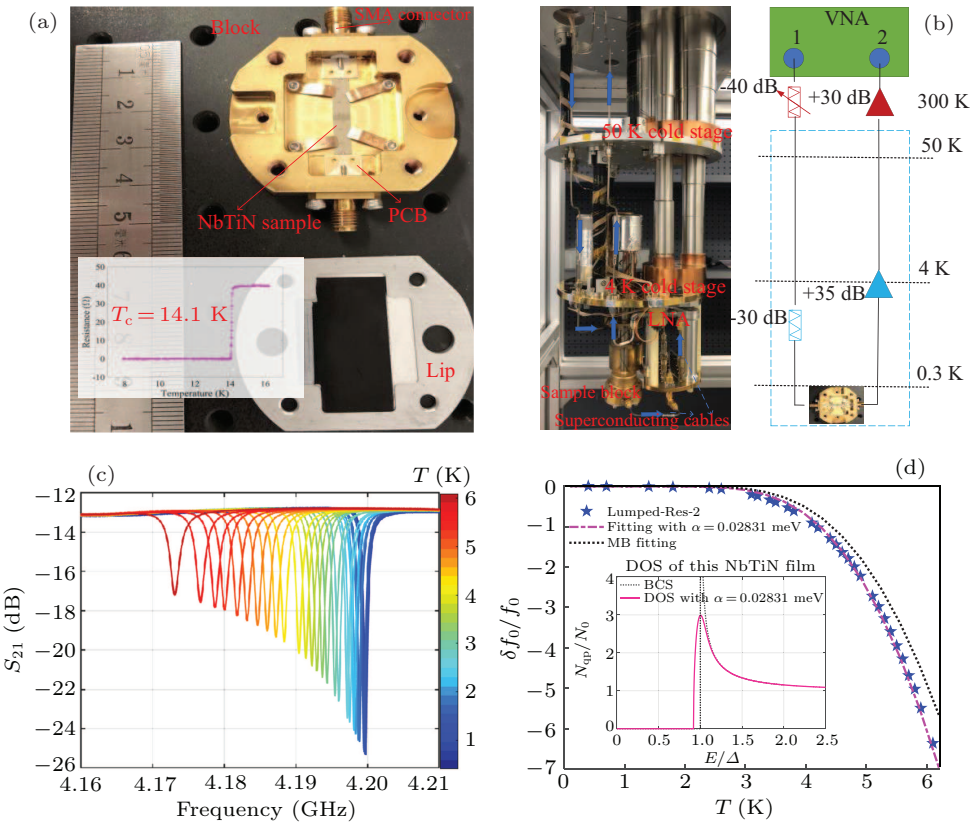


Fig. 5. (a) A photograph depicting the connection and assembly of the sample chip within the block. (b) Visual representation of the sample block's installation within the absorption refrigerator, together with a schematic diagram outlining the testing methodology. (c) Typical characteristics of one of the resonators, the absorption dip for different temperatures. (d) The relationship between the normalized resonant frequency of the resonator and the temperature.

Consequently, the numerical simulations and the parameters of the superconducting film enable the prediction of the temperature-dependent variation of the resonant frequency of a superconducting resonator made of disordered materials. Figure 5(d) illustrates our experimental and numerical simulated results for the temperature-dependent relations of resonance frequencies. The experimental results are shown in blue stars, while the numerical simulated results are shown in pink dotted lines. In contrast, the black dotted line indicates the numerical simulated results using BCS theory. It can be seen that for our NbTiN sample with disorder effects, our numerical simulations that take the Usadel equation into consideration are more consistent with the experimental results. Based on our simulations and fitting results, the pair-breaking parameter α of our NbTiN sample is determined at 0.02831 meV, also corresponding to $0.013 \cdot \Delta^{\mathrm{P}}(0)$ in our film, and the kinetic inductance fraction is 0.22. The inside figure in Fig. 5(d) gives the QDOS distribution of our NbTiN sample. Note that the measured T_{c} of 14.1 K reflects the T_{c} under disorder effects. Thus, by incorporating the value of α obtained for the NbTiN sample and by examining the relationship between the T_{c} and α, the critical temperature in a pure state $T_{\mathrm{c}}^{\mathrm{P}}$ of our NbTiN sample is characterized at 14.359 K.

5. Conclusion

We have presented numerical simulations and discussions of the disorder effects on the basic parameters of the superconducting thin film, such as QDOS, the Δ, T_{c}, and complex conductivity. To validate our theoretical study and numerical simulations, we have fabricated and characterized a superconducting planar resonator composed of the NbTiN film. The disorder-induced pair-breaking parameter $\alpha = 0.02831$ meV and the critical temperature in the pure state $T_{\mathrm{c}}^{\mathrm{P}} = 14.359$ K of our NbTiN sample are successfully characterized via numerical simulations and experimental results. This study should be applicable for the characterization and optimization of superconducting resonators in the presence of disorder effects.

Acknowledgements

Project supported by the National Natural Science Foundation of China (Grant Nos. 11925304 and 12020101002) and the Chinese Academy of Sciences Program (Grant No. GJJSTD20210002).

References

[1] Karpov A, Miller D, Rice F, Stern J A, Bumble B, LeDuc H G and Zmuidzinas J 2007 *IEEE Trans. Appl. Supercond.* **17** 343
[2] Li J, Takeda M, Wang Z, Shi S C and Yang J 2008 *Appl. Phys. Lett.* **92** 222504
[3] Jiang L, Shiba S, Shiino T, Shimbo K, Sakai N, Yamakura T and Yamamoto S 2010 *Superconductor Science and Technology* **23** 045025
[4] Leduc H G, Bumble B, Day P K, Eom B H, Gao J, Golwala S, Mazin B A, McHugh S, Merrill A, Moore D C, Noroozian O, Turner A D and Zmuidzinas J 2010 *Appl. Phys. Lett.* **97** 102509
[5] Barends R, Hortensius H L, Zijlstra T, Baselmans J J A, Yates S J C, Gao J R and Klapwijk T M 2008 *Appl. Phys. Lett.* **92** 223502
[6] Samkharadze N, Bruno A, Scarlino P, Zheng G, DiVincenzo D P, DiCarlo L and Vandersypen L M K 2016 *Phys. Rev. Appl.* **5** 044004
[7] Driessen E F C, Coumou P C J J, Tromp R R, de Visser P J and Klapwijk T M 2012 *Phys. Rev. Lett.* **109** 107003
[8] Bueno J, Coumou P C J J, Zheng G, de Visser P J, Klapwijk T M, Driessen E F C, Doyle S and Baselmans J J A 2014 *Appl. Phys. Lett.* **105** 192601
[9] Cheng B, Wu L, Laurita N J, Singh H, Chand M, Raychaudhuri P and Armitage N P 2016 *Phys. Rev. B.* **93** 180511
[10] Hazra D, Tsavdaris N, Mukhtarova A, Jacquemin M, Blanchet F, Albert R, Jebari S, Grimm A, Konar A, Blanquet E, Mercier F, Chapelier C and Hofheinz M 2018 *Phys. Rev. B* **97** 144518
[11] Skalski S, Betbeder-Matibet O and Weiss P R 1964 *Phys. Rev.* **136(6A)** A1500
[12] Gantmakher V F and Dolgopolov V T 2010 *Physics-Uspekhi* **53** 1
[13] Sacépé B, Chapelier C, Baturina T I, Vinokur V M, Baklanov M R and Sanquer M 2010 *Nat. Commun.* **1** 140
[14] Gueron S 1997 *Quasiparticles in a diffusive conductor: Interaction and pairing* Ph. D. Dissertation (Université Pierre et Marie Curie-Paris)
[15] Eilenberger G 1968 *Zeitschrift für Physik A Hadrons and nuclei* **214** 195
[16] Usadel K D 1970 *Phys. Rev. Lett.* **25** 507
[17] Wang G, Barry P S, Cecil T, Chang C L, Li J, Lisovenko M and Zhang J 2023 *IEEE Trans. on Appl. Supercond.* **33** 1
[18] Mattis D C and Bardeen J 1958 *Phys. Rev.* **111** 412
[19] Nam S B 1967 *Phys. Rev.* **156** 487
[20] Feigel'man M V and Skvortsov M A 2012 *Phys. Rev. Lett.* **109** 147002
[21] Coumou P C J J 2015 *Electrodynamics of strongly disordered superconductors* Ph. D. Dissertation (Kavli Institute of Nanoscience Delft)
[22] Belzig W, Wilhelm F K, Bruder C, Schön G and Zaikin A D 1999 *Superlattices Microstruct.* **25** 1251
[23] Sacépé B, Chapelier C, Baturina T I, Vinokur V M, Baklanov M R and Sanquer M 2008 *Phys. Rev. Lett.* **101** 157006
[24] Abrikosov A A and Gor'kov L P 1960 *Zhur Eksptl Teor. Fiz* **39** 1781
[25] Mackenzie A P, Haselwimmer R K W, Tyler A W, Lonzarich G G, Mori Y, Nishizaki S and Maeno Y 1998 *Phys. Rev. Lett.* **80** 161
[26] Gao J 2008 *The physics of superconducting microwave resonators* Ph. D. Dissertation (California Institute of Technology)